



Beyond the word and image: II- Structural and functional connectivity of a common semantic system



A.L. Jouen^a, T.M. Ellmore^b, C.J. Madden-Lombardi^a, C. Pallier^c, P.F. Dominey^a, J. Ventre-Dominey^{a,*}

^a Univ Lyon, Université Claude Bernard Lyon 1, Inserm, Stem Cell and Brain Research Institute U1208, 69500 Bron, France

^b Department of Psychology and Program in Cognitive Neuroscience, The City College and Graduate Center of the City, University of New York, New York, NY, USA

^c Cognitive Neuroimaging Unit, INSERM-CEA, Gif-sur-Yvette, France

ARTICLE INFO

Keywords:

Diffusion tensor imaging- functional interaction
Multimodal
Cognitive functions- semantic framework- human

ABSTRACT

Understanding events requires interplaying cognitive processes arising in neural networks whose organisation and connectivity remain subjects of controversy in humans. In the present study, by combining diffusion tensor imaging and functional interaction analysis, we aim to provide new insights on the organisation of the structural and functional pathways connecting the multiple nodes of the identified semantic system -shared by vision and language (Jouen et al., 2015). We investigated a group of 19 healthy human subjects during experimental tasks of reading sentences or seeing pictures. The structural connectivity was realised by deterministic tractography using an algorithm to extract white matter fibers terminating in the selected regions of interest (ROIs) and the functional connectivity by independent component analysis to measure correlated activities among these ROIs. The major connections link ventral neural structures including the parietal and temporal cortices through inferior and middle longitudinal fasciculi, the retrosplenial and parahippocampal cortices through the cingulate bundle, and the temporal and prefrontal structures through the uncinate fasciculus. The imageability score provided when the subject was reading a sentence was significantly correlated with the factor of anisotropy of the left parieto-temporal connections of the middle longitudinal fasciculus. A large part of this ventrally localised structural connectivity corresponds to functional interactions between the main parietal, temporal and frontal nodes. More precisely, the strong coactivation both in the anterior temporal pole and in the region of the temporo-parietal cortex suggests dual and cooperating roles for these areas within the semantic system. These findings are discussed in terms of two semantics-related sub-systems responsible for conceptual representation.

Introduction

Understanding the world constitutes a human aptitude that requires high-order semantic operations realized in distributed neural networks. A number of studies have been conducted to investigate the organisation of such semantic systems in healthy humans and neurological patients- for review see (Binder et al., 2009; Lambon Ralph et al., 2017). By neuroimaging meta-analyses (Binder et al., 2009), the existence of a large-scale network involved in language comprehension has been described in a set of left lateralized ventral regions widely distributed between the parietal, temporal and prefrontal cortices as well as the medial structures (parahippocampus, posterior cingulate, ventro-medial prefrontal cortex). By using verbal and non verbal tasks, multimodal integration or semantic processing have been investigated in patients

(Bozeat et al., 2000; Jefferies and Lambon Ralph, 2006) and in normal subjects during fMRI (Vandenberghe et al., 1996; Visser and Lambon Ralph, 2011) and TMS (Pobric et al., 2010) explorations. In a recent report, we have identified a semantic network which was commonly activated during tasks of image and sentence comprehension (Jouen et al., 2015). Our findings suggest that the connections between inferior parietal cortex and anterior temporal cortex might play a key role in such a multimodal semantic representation. Accordingly, compelling evidence on a role of the temporal lobe in semantic processes has been provided by clinical observations in patients with anterior temporal lobes atrophy (Lambon Ralph, 2014; Patterson et al., 2007; Rice et al., 2015). These patients have a significant and progressive loss of semantic capabilities concerning linguistic as well as other sensory modalities (vision, auditory). Moreover, by diffusion-weighted imaging tractography, Binney

* Corresponding author. INSERM Stem Cell and Brain Research Institute, U846, 18 Avenue Doyen Lepine, 69500 Bron, France.
E-mail address: Jocelyne.ventre-dominey@inserm.fr (J. Ventre-Dominey).

et al., (2012) described how the temporal lobe may contain a caudo-rostral gradient of sensory features converging from modality specific encoding in the caudal regions to transmodal representation in the middle and rostral temporal regions. The authors suggest that corresponding bottom-up and top-down interactions should co-exist dynamically.

While the neural network underpinning semantic cognition has been well described especially in the language domain, the white matter connectivity responsible for the interregional communication among nodes of the network remains a matter of debate. In humans the traditional post-mortem fiber dissection allowed scientists to identify the major white matter fascicle trajectories with no precise termination of the fiber limits. More recently, the tractography technique based on diffusion tensor imaging (Le Bihan et al., 1986) offers an in vivo and noninvasive way to determine the associative pathways connecting the largely distributed brain regions. In the domain of semantic cognition, early tractography studies concerned the language system with the description of left lateralized parallel temporo-parieto-frontal pathways involved in speech production and comprehension (Catani et al., 2005; Glasser and Rilling, 2008; Hagmann et al., 2006; Hickok and Poeppel, 2004; Makris and Pandya, 2009; Powell et al., 2006). Such a two-route language connectivity includes (1) a direct dorsal temporo-frontal pathway made of the prominent arcuate fasciculus connecting Wernicke's area involved in speech comprehension and Broca's area involved in speech production, and (2) an indirect ventral pathway connecting the parietal lobe to Wernicke's area (posterior segment) and to Broca's area (anterior segment) (Catani et al., 2005; Parker et al., 2005; Saur et al., 2008). Consistent with the original post-mortem description, this left-lateralized white matter structural organisation of the language system has been further confirmed and developed by using -probabilistic DTI in normal or brain-damaged subjects (Binney et al., 2012; Ellmore et al., 2010; Fang et al., 2015; Floel et al., 2009; Han et al., 2013), -combined functional and anatomical connectivity (Saur et al., 2010) or -direct electrical stimulation for intraoperative mapping (Almairac et al., 2015; De Witt Hamer et al., 2011; Duffau et al., 2013). By combining anatomical and functional findings in human, Ueno et al., (2011) built a computationally-implemented model, of the dual pathways that provides a platform for simulation of language semantic processing.

Therefore, the dual stream model has been extended with functional descriptions suggesting multiple components of the ventral semantic pathways: the direct inferior fronto-occipital fasciculus (iFOF), the middle (mLF) and inferior (iLF) longitudinal fasciculi as well as the uncinate fasciculus (UF). The role of these different white matter bundles is not well defined in terms of their relative roles in semantic function. Based on the Hickok and Poeppel model (Hickok and Poeppel, 2004), the lexical-semantic area situated between Wernicke's area, primary auditory and visual associative cortex is likely implicated in associating multimodal information to concepts. The resulting semantic information should hence be conveyed to the anterior temporal pole and inferior frontal cortex across the middle temporal pathways as suggested in the literature (Glasser and Rilling, 2008; Jefferies, 2013; Jung et al., 2016; Lambon Ralph et al., 2017; Noonan et al., 2010; Saur et al., 2010). First, neuroimaging studies converge to the idea of complementary contributions in language comprehension of each one of these ventral tracts. The iLF might be involved in mediating lexical semantic information to be integrated and stored in the anterior temporal lobe (Saur et al., 2010; Wei et al., 2012), while the UF would be involved in modulating this conceptual representation by cognitive control mechanisms issued from the inferior prefrontal cortex (Harvey et al., 2013; Saur et al., 2010). Parallel and dorsal to the iLF, the mLF recently discovered in human constitutes a large tract of long-distance white matter fibers running in the superior temporal lobe from the posterior cortical regions to the anterior regions of the temporal lobe (Makris et al., 2009, 2017). Because of these large inter-regional connections, the mLF has been implicated in a variety of cognitive functions including language, visuospatial and attentional processes as well as high order multimodal association functions (Makris et al.,

2017). Finally, based on a series of brain electrostimulation studies in patients, Duffau's team proposes the iFOF as the essential pathway for multimodal semantic processing (Almairac et al., 2015; Duffau et al., 2013; Moritz-Gasser et al., 2013). Like the mLF, the iFOF constitutes a long, multiregional association pathway running through the extreme capsule and connecting the occipital, parietal and postero-lateral temporal cortical areas to the prefrontal cortex including the orbito-frontal and dorsolateral regions (Catani and Thiebaut de Schotten, 2008; Martino et al., 2010). Based on their observations, Duffau and colleagues (Duffau et al., 2013) propose a dual stream model of the ventral connectivity constituted by (1) a direct multicomponent route, the iFOF involved in semantic knowledge, and (2) a secondary indirect route made of iLF and UF (and possibly the mLF), involved in compensable semantic processing. However, while the literature is converging on the structural description of the different ventral white matter pathways, their respective roles in semantic processing remain a matter of controversy, particularly in the domain of the connectivity underlying transmodal conceptualization.

We build on a previous fMRI neuroimaging research in healthy humans where we have identified a semantic network of neural structures commonly activated for pictures and sentences (Jouen et al., 2015). This network forms a ventral neural system largely distributed between lateral (parieto-temporal and prefrontal) and medial (prefrontal, cingulate and parahippocampal) cortical regions with emphasis on the role of the parieto-temporal region as a hub for heteromodal semantic operations. In the present study, by combining diffusion tensor imaging and functional interaction analysis, we aim to provide new insights on the organisation of the structural and functional pathways connecting the multiple nodes of the identified semantic system -shared by vision and language. Indeed, while the majority of studies investigating semantic network connectivity focus on language comprehension or on localized neural structures, we will attempt to characterize a global framework for semantic processing common to language and visual scenes and grounded on both neural and functional connectivity, including long range connections. In order to investigate such an organisation of structural and functional connections underlying an effective interregional communication, we used as seeds the regions of interest (ROIs) identified in the semantic network common to language and visual scene processing (Jouen et al., 2015). The anatomical and functional connectivity was explored respectively by deterministic tractography to isolate only the fibers terminating in the selected ROIs and by independent component analysis (ICA) to extract the significant correlations between activated areas.

Material and methods

The methods and the experimental paradigm have been previously described in an event-related fMRI investigation of conceptual processes shared between images and sentences (Jouen et al., 2015). The unique features of the methods for the novel analyses of this study are reported here.

Subjects

Nineteen healthy young right-handed subjects participated in this study (11 males, mean age = $23,05 \pm 5,44$, age range: 18–42 years). All participants were in good health with no history of psychiatric or neurological disease nor alcohol or drug abuse as established during the pre-experiment medical examination. The research protocol was approved by the local ethic committee (Ile de France Comity; Protocol # 2008-A00241-54/1) and all subjects gave their written informed consent prior to the scanning session.

Paradigm

The paradigm used in the study consisted of 200 pictures (Event pictures) and 200 sentences (Event sentences). The images are from the Getty photo database (<http://www.gettyimages.fr/>) and show typical

visual scenes of single persons (no negative emotional valence) performing common daily activities (e.g. reading, running, raking leaves, eating). The sentences described the same actions and were generated such that the sentences corresponded to an equivalent set of events as the pictures (e.g., “The woman buys herself a new jacket.” “The little boy runs in the yard.”). Two sets of stimuli (A and B) were generated, each composed of 100 pictures and 100 sentences (see Supplementary material: [SM-Table 1](#) for norming data on the sentence stimuli). In order to avoid subjects seeing both a given sentence and its corresponding picture, stimuli were crossed, such that the 100 sentences in stimulus set A corresponded to the 100 pictures from stimulus set B and vice versa. So as to subtract low-level (non-semantic) processing in subsequent analyses, Control pictures (25) were generated as scrambled images from the original pictures, and Control sentences (25) were generated as scrambled strings of letters from the original sentences. The subjects' task was to silently read the sentences, and silently view the images, and they were asked to process the stimuli in a natural way, as if they were reading for pleasure or looking through pictures in a magazine. In order to maintain subjects' alertness, 10% of trials were followed by a picture or a sentence and a question asking if the current stimulus had previously been seen. The subject had to respond with their right hand by pressing on a button pad, and if the correct response was positive (as on 50% of question trials), the previous occurrence was always one-back. The number of correct responses to subjects' accuracy on these questions exceeded 95% indicating that the subjects were attending to the stimuli. Our previous study using the same paradigm ([Jouen et al., 2015](#)), demonstrates that the image and sentence stimuli effectively engage the desired semantic processing.

During the fMRI scanning session, 10 subjects were exposed to set A, and 9 to set B. The pictures and sentences stimuli were presented in 4 runs with each one consisting of 50 event trials, 25 control trials and 8 probe questions. During a trial, a white fixation cross appeared on a black screen for 500 ms, followed by a picture or sentence on a black background for 2 s, and finally a blank black screen was presented for 2 s plus jitter time (0–6 s) before the next trial.

Following the scanning, the subjects' imageability capability was assessed during a behavioral test on a subset of 50 sentences: 25 from the list that they had just seen in the scanner, and 25 from the list that the other half of subjects saw. Subjects were instructed to rate how well they were able to visualize the sentence, or how vivid their representation was. For this purpose, they had to provide judgments of visual imageability (Imageability score = IS) using a subjective scale, from 1 the lowest to 5 the highest imageability score.

Procedure

Functional and structural MRI data were acquired on a 3T Siemens Magnetom TrioTim scanner at Neurospin (CEA Saclay, Gif-sur-Yvette, France). Blood oxygen level dependent (BOLD) fMRI signal was recorded during the four experimental runs. Whole brain coverage was obtained with 38 transversal gradient echo-planar imaging (EPI) images (repetition time: 2000 ms, echo time: 30 ms, flip angle: 76°, bandwidth: 2694 Hz per pixel, FOV: 192 mm², voxel size: 3.0 mm³, 300 repetitions). A high resolution T1 weighted image of the whole brain was acquired for later spatial coregistration (TR/TE: 2300/2.98 ms; flip angle: 9°; FOV: 256 mm²; 1.10 mm thick sagittal slices). During the same session, 3 successive scans of 19, 20 and 21 distinct direction diffusion gradients were acquired so as to form a concatenated 60 direction diffusion image, to allow reconstruction of white matter pathways (TR/TE: 13000/93 ms; flip angle: 90°; matrix size: 128 × 128; FOV: 220 mm²; 1.70 mm thick axial slices, max. b-value: 1500 s/mm²).

Data analysis

DTI data analysis

The image processing, re-alignment and visualization were

performed with the AFNI software ([Cox, 1996](#)). Each diffusion weighted volume in each of the three DTI runs was aligned to the subject's skull-stripped T1 weighted MRI using AFNI's 3dAllineate with mutual information as the cost function. Separately, the T1 MRI was spatially normalized to the MNI template (Montreal Neurological Institute N27 brain) and the resulting 12-parameter affine transformation matrix was saved. The angular motion parameters calculated were used to rotate each of the three sets of gradient directions to adjust for subject motion relative to the scanner gradient axes ([Leemans and Jones, 2009](#)). The three sets of aligned diffusion-weighted volumes were then concatenated using AFNI's 3dTcat function to make one 3d + time diffusion weighted brik containing all the aligned diffusion weighted volumes collected during the imaging session. A single tensor was then computed using AFNI's 3dDWItoDT using as input the single concatenated diffusion brik and the concatenated gradient directions, which were adjusted for angular motion. The single tensor output previously obtained was then used as input to compute the individual set of whole brain tracts for each subject. A set of whole-brain deterministic pathways was saved in a pathway database for further exploration. The gradient scheme is illustrated in the supplementary material ([SM-Fig. 1](#)).

The native-space resolution of the output realigned diffusion-weighted volumes (1.72 × 1.72 × 1.70 mm) was preserved for the purposes of computing the set of whole-brain tractography pathways (no Talairach transformation). Deterministic fiber tracking was used to compute a native-space tensor in DTIQuery v1.1 software ([Sherbondy et al., 2005](#)) with the streamline tracking algorithm (STT) and optimal parameters ([Basser et al., 2000](#)), including path step size of 1.0 mm, seed point spacing at 2.0 mm, fractional anisotropy termination threshold of 0.15, angular termination threshold at 45°, maximum pathway length at 300 mm, and Euler's method for STT numerical integration.

The seed regions for the deterministic fiber tracking were extracted from the t-maps of the fMRI random effects obtained in a previous neuroimaging study ([Jouen et al., 2015](#)). Based on Nichols' conjunction analysis procedure ([Nichols et al., 2005](#)), we have identified the semantic neural network commonly activated for image and sentence in the subjects' group. This neural network is composed of a set of 13 activated regions of interest (ROIs) defined and localized by the coordinate of the local maxima “peak” within a cluster of voxels in Talairach coordinates ([Fig. 1](#)): on the lateral walls, the left and right inferior Parietal lobe (iP-BA39), the left superior Temporal gyrus (sT-BA22), the left and right middle Temporal gyrus (mT-BA21), the left superior Temporal Pole (sTP-BA38), the left inferior PreFrontal gyrus (iPF-BA45,46) and the left middle PreFrontal gyrus (mPF-BA6); on the medial walls, the left posterior Cingulum or RetroSplenial cortex (RSC-BA29-30), the left para-Hippocampal gyrus (pH-BA35), the left and right ventro-medial PreFrontal gyrus (vmPF-BA11) and the caudate nucleus.

The anatomical characteristics of the 13 ROIs used as the seeds are shown in [Table 1](#). Sets of tractography pathways were objectively isolated using the following steps: 1) a backward transformation of the local maxima coordinates from the fMRI group ROIs map was performed for each subject to obtain a native image space coordinate; 2) these individual coordinates were used to place volumes of interest in DTI Query (VOI = sphere centered on a ROI peak voxel with a radius of 10 mm); 3) the pathways terminating in the different VOIs pairs were saved as a native space binary image volume for each subject. The AFNI tractography algorithm computed only fibers terminating in the VOIs seeds, excluding passing fibers because of the uncertainty of their terminations. In each separate hemisphere, we identified the pathways connecting pairs of (a) the 7 left VOIs (iP, sT, mT, sTP, iPF, mPF, vmPF), (b) the 3 medial VOIs (RSC, pH, Caudate) and (c) the 3 right VOIs (iP, mT, vmPF). A total of 57 possible bundles by subject was computed with 42 bundles connecting the left and medial VOIs pairs, 12 connecting right and medial VOIs pairs and 3 connecting the medial VOIs pairs to each other. Then this native space image was transformed to MNI space using the 12-parameter transformation matrix derived from the T1 MRI spatial normalization procedure. This resulted in 19 single-subject image

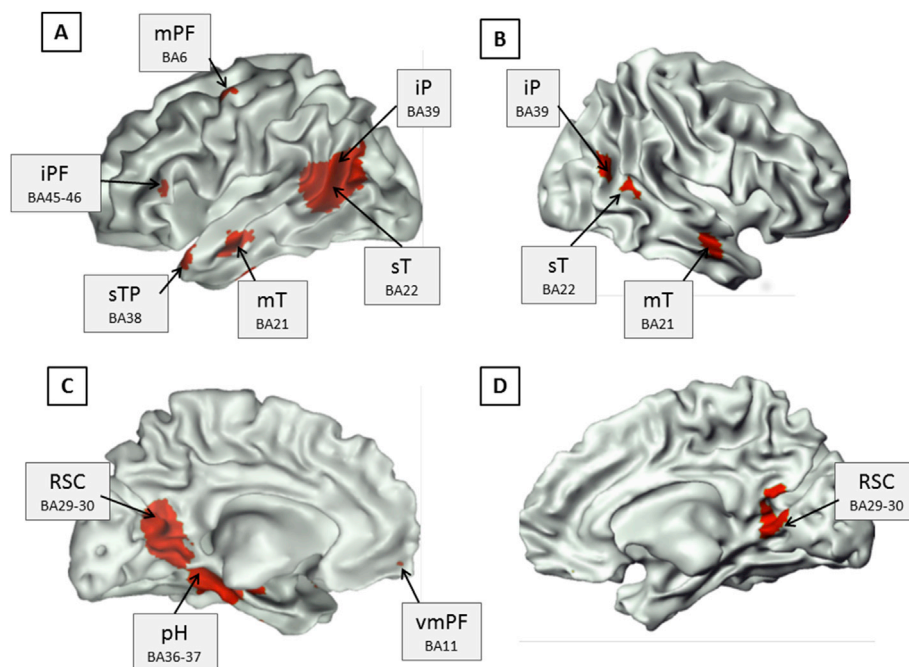


Fig. 1. Lateral and medial views of the brain representing the identified semantic network shared by pictures and sentences processes. ROIs in the lateral left (A) and right (B) sides: Inferior prefrontal cortex (iPF)- middle prefrontal cortex (mPF)-Superior and middle temporal cortices (sT,mT)- Superior temporal pole (sTP)- Inferior parietal cortex (iP). ROIs in the medial left (C) and right (D) sides: retrosplenial cortex (RSC),parahippocampal cortex (pH) and ventro-medial frontal cortex (vmPF). Each ROI is identified with the corresponding Brodman's area. Adapted with permission from Jouen et al. (2015).

Table 1

ROIs anatomical regions used as seeds for fiber tractography. Anatomical localization and coordinates are based on Talairach and Tournoux's stereotaxic atlas (1988).

| ROI-Anatomical area | BA | Tal x, y, z | Peak t value |
|--|-----------|--------------|--------------|
| L Parahippocampal Gyrus (pH) | 35/ 36 | -33, -38, -8 | 6.63 |
| L Cingulum post (RSC) | 29/ 30 | -9, -55, 17 | 5.52 |
| L Inferior Parietal Lobe (iP) | 39 | -42, -66, 23 | 6.64 |
| L Superior Temporal Gyrus (sT) | 22 | -53, -52, 14 | 5.72 |
| R Inferior Parietal Lobe (iP) | 39 | 53, -69, 26 | 3.89 |
| L Middle Temporal Gyrus (mT) | 21 | -63, -4, -15 | 4.43 |
| R Middle Temporal Gyrus (mT) | 21 | 53, -7, -17 | 4.39 |
| L Superior Temporal Pole (sTP) | 38 | -45, 16, -21 | 3.84 |
| R Ventro-Medial Prefrontal Cortex (vmPF) | 11 | 3, 40, -17 | 3.13 |
| L Ventro-Medial Prefrontal Cortex (vmPF) | 11 | -9, 52, -13 | 3.16 |
| L Inferior Prefrontal Gyrus (iPF) | 45/ 46 | -56, 29, 7 | 3.41 |
| L Middle Prefrontal Gyrus (mPF) | 6 | -42, 0, 53 | 3.00 |
| R Caudate | | 3, 11, -6 | 3.04 |

volume masks in the same standard coordinate space. These volumes were then summed to create a single volume map where the integer value at each voxel represents the number of subjects who have tractography pathways passing through the given voxel. A threshold was applied to this volume to visualize voxels where at least 10 of the 19 subjects exhibited common tractography connections.

The tractography connections were quantified with the factor of anisotropy (FA), the number of fibers and the percentage of fibers (ratio of the number of fibers for one tract to the number of the whole brain fibers for one subject) for each determined pathway. The tractography parameters were correlated to mean imageability ratings by using a correlation factor analysis on the main identified pathways. The significance level was established at 95% confidence interval.

Independent component analysis of fMRI data (NetbrainWork)

To determine functional connectivity between activated regions we

used the NetBrainWork software (<https://sites.google.com/site/netbrainwork/>) (Coynel et al., 2010; Perlberg et al 2008, 2009). For each participant and each run, imaging data were first processed using an independent component (IC) analysis (infomax ICA algorithm) that reduced the data to the 40 components explaining the most variance. These individual ICs were scaled to z-scores and normalized into MNI standard stereotaxic space. All the individual ICs were pooled across participants separately for Images and Sentences condition and then clustered on their spatial similarities to form "classes" of interest (COIs). This partitioning was automatically realized by NetBrainWork using criteria to optimize both the Unicity and Representativity of each COI. The degree of Representativity indicates that each participant is represented with at least one component in a given COI and the degree of Unicity indicates that one participant contributes to a COI with only one component. As these criteria should ideally equal 1, we retained only COIs with Representativity and Unicity >0.75 that corresponded to 3 COIs for each condition. For each COI, fixed effect analyses were computed to extract t-scores maps with a Bonferroni correction thresholded at $p \leq 0.01$ with a minimal extension cluster of 10 voxels.

By visual inspections of the COIs, the ROIs overlapping the common nodes (the 13 ROIs selected as the DTI seeds as described above) were selected for further functional connectivity computed separately for each Image and Sentence condition. The degree of overlap between ROIs and the two image and sentence COIs was calculated by the following equation: $\text{overlap \%} = \text{COI} \cap \text{ROI surface} \times 100 / \text{ROI surface}$ ($\text{COI} \cap \text{ROI} = \text{Intersection between ROI and COI}$). Once the networks were identified and after noise correction, pairwise correlations between the time-course of each ROI were estimated for each separated Image and Sentence network. Significant marginal and partial correlations were established at $p < 0.05$ with Bonferroni corrections for multiple comparisons. In contrast to the marginal correlation, the partial correlation indicates the covariance between the time courses of two nodes after removal of the variance effects from other nodes. Thus the partial correlation measures the specific relation between two ROIs independently of any other influences.

A functional integration was calculated independently for each image

and sentence network. Hierarchical integration corresponds to the mutual information between time courses of BOLD signal recorded in the various ROIs (Marrelec et al., 2008; Perlberg and Marrelec, 2008). This provides a global measure of functional information exchanges within and/or between brain systems (SOIs: Systems of Interest). Furthermore, if a system is divided into subsystems like in our study Image and Sentence, the total integration of this system can be decomposed into within-subsystem and between-subsystem integration (Marrelec et al., 2008). In particular, the total integration of the brain is equal to the sum of within-SOIs integration and between-SOIs integration. To infer the integration measures, a Bayesian numerical sampling scheme approximating the posterior distribution of the parameters of interest in a group analysis is necessary. In the actual study, we used 1000 samples to perform this approximation, therefore leading to a thousand estimations of integration measures. The results are presented in terms of the mean and standard deviation of the 1000 estimates for each subsystem Image (I) and Sentence (S). The interested reader can find further information about the concept and the computation of hierarchical integration in Marrelec et al. (2008).

Results

Structural identification of the main fibers tracts

Among the fiber tracts defined with our 13 ROIs distributed between the two hemispheres, 12 tracts have been retained as they were found in at least 10 subjects (Table 2): 9 were identified in the left hemisphere, one in the medial structures between RSC and pH, and 2 were localized in the right hemisphere. Among 34 fiber tracts identified, 22 tracts were not retained for further analysis as each one was found in less than 10 subjects. The characteristics (percentage of fibers and factor of anisotropy) of these 34 tracts are provided for all subjects, in Tables 2 and 3 of the supplementary material.

As shown in Figs. 2 and 3, the left cortico-cortical pathways could be dissociated into two major ventral streams issued from the left superior temporal ROI: one (corresponding to the middle and inferior longitudinal fasciculi) running posteriorly and forming a parieto-temporal stream and another (corresponding to the uncinate fasciculus) running rostrally and forming a temporo-prefrontal stream. As part of this ventral network, we also found short connections between the retrosplenial cortex and the parahippocampal gyrus passing through the cingulum white matter (Fig. 4).

Table 2

Characteristics of the 12 main pathways identified in the semantic network and connecting the parietal, temporal and prefrontal cortices and the caudate nucleus. Number of subjects (Nb Subjects), mean percentage of fibers (%*10) and mean factor of anisotropy (FA). Standard deviations in parenthesis. mLF and iLF: middle and inferior longitudinal fasciculus; UN: uncinate fasciculus; TR: thalamic radiations; CIN: cingulate white matter.

| | mLF | | iLF | UN | | | |
|-------------|-------------|-------------|-------------|-------------|-------------|-------------|------|
| | BA21 | BA39 | BA35 | BA45 | BA11 | Caudate | |
| | Left H | |
| Nb Subjects | 12 | 11 | 13 | 10 | 15 | 14 | |
| % Fibers | 0.07 (0.05) | 0.14 (0.20) | 0.16 (0.16) | 0.05 (0.04) | 0.20 (0.13) | 0.10 (0.07) | BA38 |
| FA | 0.28 (0.07) | 0.44 (0.03) | 0.39 (0.06) | 0.41 (0.05) | 0.40 (0.02) | 0.36 (0.04) | |
| | mLF | | CIN | TR | | | |
| | BA21 | BA22 | BA35 | Caudate | | | |
| | Left H | Right H | Left H | Left H | Right H | | |
| Nb Subjects | 11 | 15 | 18 | – | – | – | |
| % Fibers | 0.18 (0.31) | 0.22 (0.24) | 0.17 (0.14) | – | – | – | BA39 |
| FA | 0.44 (0.03) | 0.44 (0.02) | 0.35 (0.04) | – | – | – | |
| | | | | | | | |
| | | | | | | | |
| | | | | | | | |
| Nb Subjects | – | – | – | 12 | – | – | |
| % Fibers | – | – | – | 0.08 (0.10) | – | – | RSC |
| FA | – | – | – | 0.35 (0.07) | – | – | |
| | | | | | | | |
| | | | | | | | |
| | | | | | | | |
| Nb Subjects | – | – | – | – | 17 | 18 | |
| % Fibers | – | – | – | – | 0.18 (0.20) | 0.32 (0.22) | BA11 |
| FA | – | – | – | – | 0.31 (0.05) | 0.26 (0.06) | |

As illustrated in Fig. 2, the parieto-temporal stream is represented by a large bundle of white matter (WM) fibers running through the temporal lobe. On coronal sections posterior to the left Heschl transverse gyrus, we could distinguish two clusters of high WM density dorso-ventrally superposed and likely corresponding dorsally to the middle (mLF) and ventrally to the inferior (iLF) longitudinal fasciculi. In the inferior parietal lobe, the mLF was observed with two branches originating from the two banks of the superior temporal sulcus, corresponding to the inferior parietal (BA39) and superior temporal (BA22) cortices. It then ran along the depth of the superior and middle temporal lobes and at the level of the posterior extremity of the hippocampus, coursed along the superior temporal lobe before reaching the anterior temporal pole (BA38). In contrast, the more ventral fibers came from the parahippocampus and fusiform cortical regions and ran in the depth of the inferior temporal lobe. The majority of these fibers reached the middle temporal cortex (BA21) and the others reached the anterior pole (BA38) through a less dense bundle. These WM hippocampo-temporal connections likely correspond to the iLF even though the WM fibers were difficult to isolate between mLF and iLF when ending at the anterior extremity of the temporal lobe.

In the right hemisphere, similar WM bundles were found to connect the inferior parietal cortex (BA39) and the middle temporal cortex (BA21) by running in the depth of the middle temporal lobe. This right ventral parieto-temporal stream likely corresponds to the inferior longitudinal fasciculus rather than to the middle fasciculus usually localized more dorsally in the superior temporal lobe.

The other stream connected the ROI of the superior temporal gyrus (BA38) and the prefrontal cortex via the uncinate fasciculus. As shown in Fig. 3, the uncinate fibers issued from the anterior temporal pole (BA38) ran in a postero-dorsal direction in the temporal lobe to make a loop before reaching two target sites: the inferior prefrontal cortex (BA45) laterally and the ventro-medial prefrontal cortex (BA11) medially. At the level of the anterior commissure, the uncinate bundle aimed upwards along the amygdala toward the ventral edge of the basal ganglia. At TAL -30 11 -11 it divided into two branches, one passing medially under the ventral bank of the putamen and the other continuing dorsally along the lateral bank of the putamen in the external/extreme capsule. This lateral branch joins the frontal lobe and at about TAL -30 24 17 orients laterally to the inferior prefrontal gyrus before reaching its final target, the inferior prefrontal cortex (BA45-46). This division of the uncinate WM is shown in Fig. 3B on the coronal section Y = -11. The medial branch continued rostrally along the ventral bank of the putamen to join the

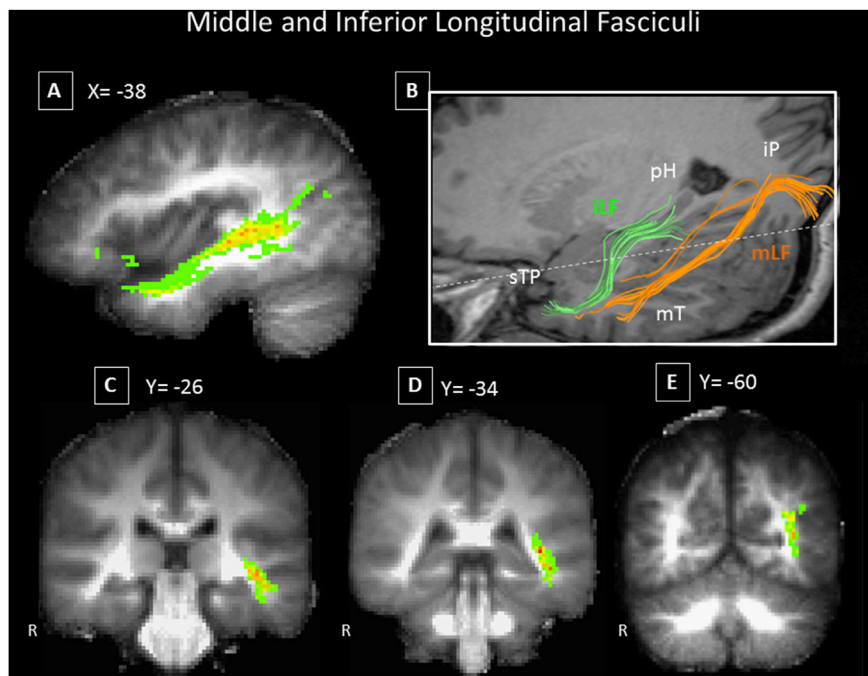


Fig. 2. Group-averaged (A, C–E) and individual (B) connections of the middle (mT = BA21) and the superior (sTP = BA38) temporal cortex -with the inferior parietal (iP = BA39) cortex via the middle longitudinal fasciculus (mLF) and -with the parahippocampus (pH) cortex via the inferior longitudinal fasciculus (iLF). Representation of group-averaged connections on sagittal (A) and coronal (C–E) views in Talairach coordinates (Talairach and Tournoux, 1988). B: 3D representation of individual mLF (in orange) and iLF (in green). The dotted line delineates the intersection between sagittal and horizontal planes.

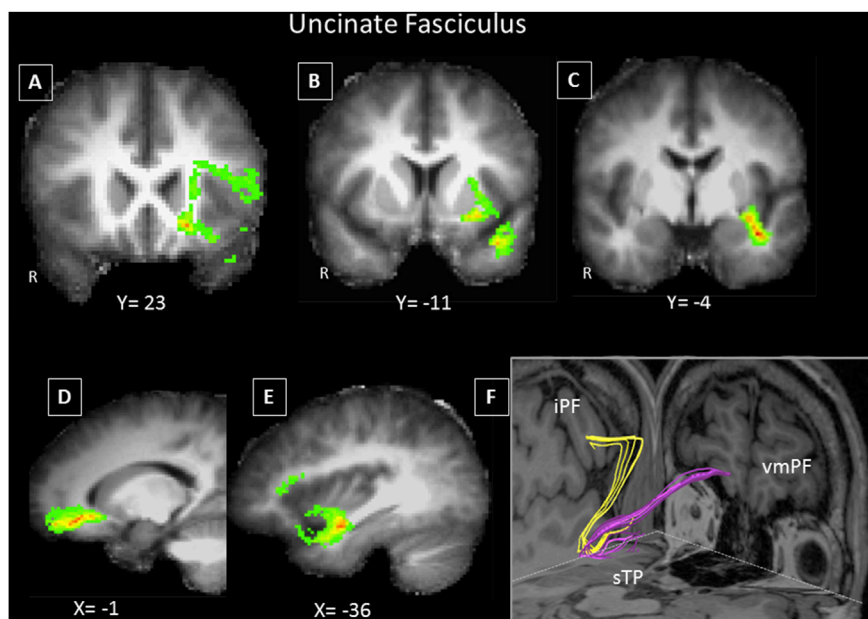


Fig. 3. Group-averaged (A–E) and individual (F) connections of the superior temporal pole (sTP = BA38) -with the inferior prefrontal (iPF = BA45) and -the ventro-medial prefrontal (vmPF = BA11) cortex via the uncinate fasciculus. Representation of group-averaged connections on coronal (A–C) and sagittal (D,E) views in Talairach coordinates (Talairach and Tournoux, 1988). B: 3D representation of the individual uncinate fasciculus branching from the superior temporal cortex to the inferior prefrontal cortex (in yellow) and to the ventro-medial prefrontal cortex (in purple). The dotted line delineates the intersection between sagittal, coronal, and horizontal planes.

anterior cingulate cortex and then its final target the left ventro-medial prefrontal cortex (Fig. 3; Tal X = -1).

Additionally, we identified in the majority of subjects (17/19 on the left and 18/19 on the right) subcortical projections from the ventro-medial region of the caudate nucleus to the ventro-medial prefrontal cortex through anterior thalamic radiations (Fig. 4). In 14 subjects (SM-Table 2), we could distinguish WM fibers passing through the

uncinate fasciculus to connect the caudate nucleus to the anterior temporal pole.

Correlations between fiber tract metrics and behavior

The inferior and middle longitudinal fasciculi are represented by pathways with the most density and highest level of anisotropy as

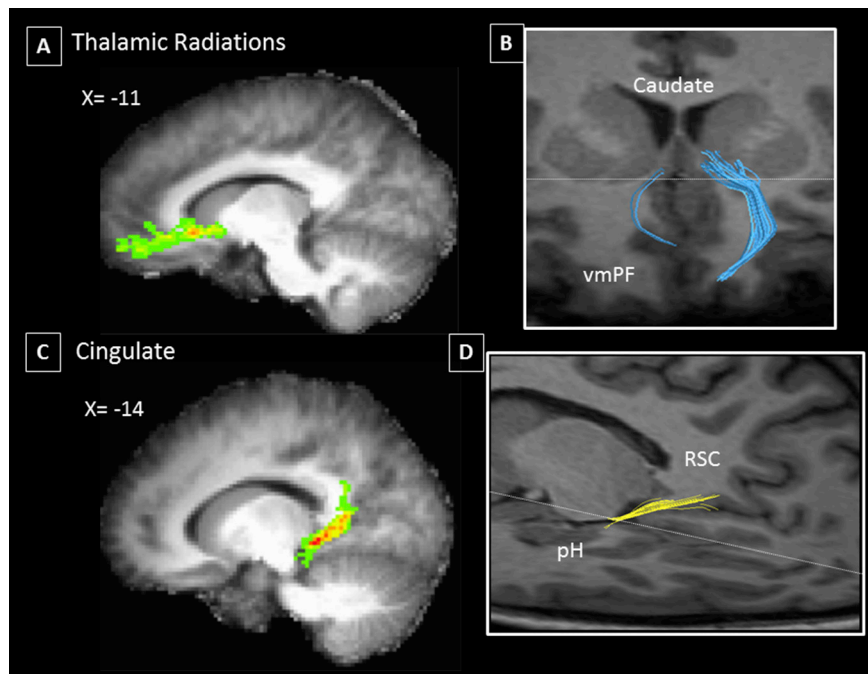


Fig. 4. (A–B) Thalamic radiations between the caudate nucleus and the ventro-medial prefrontal cortex (vmPF = BA11). (C–D) Cingulate white matter bundle between the parahippocampus (pH) gyrus and the retrosplenial cortex (RSC). (A and C) Representation of group-averaged connections on sagittal views in Talairach coordinates (Talairach and Tournoux, 1988). (B and D): 3D representation of individual connections. The dotted lines delineate the intersection (B) between coronal and horizontal planes and (D) between sagittal and horizontal planes.

compared to the other pathways of the semantic network (Table 2). Using a Pearson correlation analysis, we examined correlation between the behavioural performance (the imageability score) and metrics of the different tracts as previously described (Jouen et al., 2015). The imageability score (IS) was measured by asking subjects to rate their imageability capability when reading sentences. This IS score assessed how well they were able to visualize the sentence, or how vivid their representation was. A significant correlation between IS and FA ($r^2 = 0.60$, $p = 0.049$) was observed in this mLF bundle. Otherwise IS and FA tended to be correlated for pathways linking the parahippocampus and the superior temporal cortex (BA38) ($r^2 = 0.53$, $p = 0.065$). Only a slight correlation between IS values and % of fibers tended to occur in the left mLF connecting the inferior parietal cortex and the middle temporal cortex ($r^2 = 0.45$, $p = 0.16$).

Functional interactions in the main fiber tracts

The intrinsic activity obtained at the group level by independent component analysis (ICA) displayed a distribution quite similar to the semantic network previously defined in common for the image and sentence conditions (Jouen et al., 2015). As shown in Fig. 5, the resulting networks of COIs delimited by Netbrainwork ICA for the Image and Sentence tasks were well superimposed onto the activated semantic neural network identified with SPM t-maps in our previous study (Jouen et al., 2015). The degree of overlap between the COIs and ROIs has been quantified for each activated cerebral regions and is illustrated in the supplementary material (SM Fig. 2). A number of cortical regions were significantly activated in common between sentences and pictures and included the parieto-temporal cortex, the middle and superior temporal cortex, the middle, inferior and ventro-medial prefrontal cortex and the parahippocampus cortex, retrosplenial cortex and caudate nucleus. The functional interactions between the different nodes of such a semantic network were computed during sentences and images using either marginal or partial correlation as a measure of the functional connectivity.

The marginal pairwise correlations coefficients were highly significant ($p < 0.001$) showing positive correlations between a majority of

nodes (Fig. 6). We thus identified in each hemisphere 4 main nodes shared by sentences and images conditions: the inferior parietal, middle temporal, retrosplenial and ventro-medial prefrontal ROIs. Fig. 6 shows the matrices of the p corrected values of the marginal pairwise correlations computed between the 13 ROIs, independently for sentences and images of the semantic network. These nodes formed bilateral intermingled networks as (1) the inferior parietal node interacts significantly with the retrosplenial node, the superior and middle temporal nodes, the superior temporal pole, and the ventro-medial prefrontal node, (2) the middle temporal node with the inferior parietal node, the superior temporal pole and the ventro-medial prefrontal node, (3) the retrosplenial node with the parahippocampus node, the middle temporal and superior temporal nodes, the inferior parietal node, the ventro-medial prefrontal node and the caudate nucleus and finally (4) the ventro-medial prefrontal node with the retrosplenial node, the inferior parietal node, the middle temporal node, the superior temporal pole and the caudate nucleus. Interestingly, these matrices display a similar pattern of functional connectivity between sentences and images tasks.

As expected, when considering the partial correlations (i.e. the correlation between two nodes excluding the effect of the other nodes) the number of interactions reduced to show only the significant specific correlations. These interactions are represented in Fig. 7 as a network showing the partial correlations as links between nodes. This functional interaction analysis confirms the structural pattern of connections identified by tractography analysis previously described for both images and sentences. We note that the superior temporal pole specifically interacts with the parieto-temporal and the inferior frontal cortices and thus could be a key relay of the ventral semantic pathways. In addition, the retrosplenial cortex constitutes a central node or hub strongly interacting with several relays of the network including the bilateral ventromedial prefrontal, parieto-temporal nodes and the left parahippocampal node. In turn the ventro-medial node activity is largely connected to the parieto-temporal cortex and to the caudate nucleus on the right side. In contrast, two other nodes had a weak interaction in the network as: (1) the premotor cortex only interacted with the parieto-temporal cortex for both experimental conditions and with the inferior prefrontal cortex only for

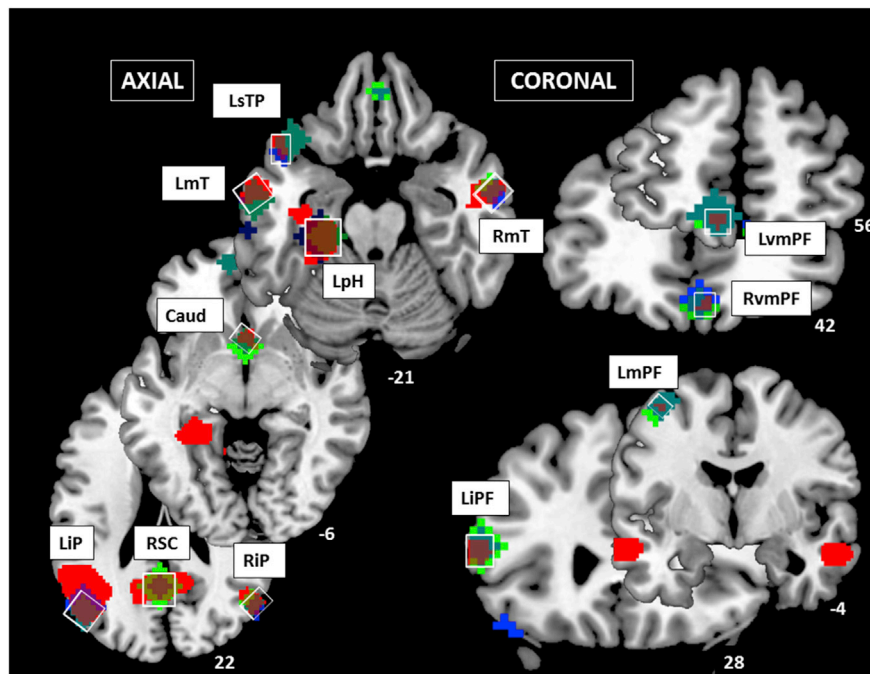


Fig. 5. Activation in the regions of interest (ROIs) determined by conjunction analysis (SPMS) in red and by independent component analysis (ICA) in blue (images) and green (sentences). Note the overlapping (brown patches) of the ROIs determined by using the different analysis methods. ROIs are represented on horizontal and coronal sections in Talairach coordinates. LiP and RiP: Left and right inferior parietal cortex-RSC: retrosplenial cortex- LmT and RmT: Left and right middle temporal cortex-LsTP: Left superior temporal pole- LpH: Left parahippocampus gyrus- LiPF: Left inferior prefrontal cortex- LmPF: Left middle prefrontal cortex- LvmPF and RvmPF: Left and right ventro-medial prefrontal cortex- Caud: Caudate nucleus.

the image condition and (2) the caudate nucleus preferentially interacted with the inferior prefrontal (inhibitory effect) and retrosplenial cortices only for sentences. Finally we found comparable levels of global hierarchical integration between sentence and image connectivity network respectively $I_s = 0.9686 \pm 0.034$ and $I_i = 1.0678 \pm 0.034$.

Discussion

Combined with our previous work (Jouen et al., 2015), these new findings provide a general framework including activated sites, their anatomical connections and functional links involved in processing meaning of sentences and images. The structural pathways are constituted of ventral white matter (WM) tracts in both hemispheres. Lateral tracts link the parieto-temporal, middle and superior temporal and inferior prefrontal sites, and medial tracts link the ventro-medial frontal cortex to the striatum and the posterior cingulate to the para-hippocampus. Analysis of the functional interactions within this semantic network revealed patterns of functional connectivity between nodes of cognitive sub-systems implicated in semantic processing that we discuss below.

The principal structural pathways of the semantic network

Here, we describe the structural correlates of the semantic network primarily including the middle and inferior longitudinal fasciculi, the uncinate fasciculus and WM fibers in the thalamic radiations and in the posterior cingulum. The principal tracts are linked to the anterior temporal pole (BA38) located in the superior temporal gyrus of the left hemisphere. As it concentrates the majority of the connections of the semantic network, this temporal region might be considered to constitute a potential hub between the posterior cortical regions and the prefrontal lobe. Such a central role of the anterior temporal lobe (ATL) in conceptualisation has been suggested in studies of semantic dementia and in neuroimaging exploration of cerebral activation and functional connectivity (Binney et al., 2012; Geranmayeh et al., 2015; Guo et al., 2013; Jackson et al., 2016; Lambon Ralph et al., 2017, Patterson et al., 2007;

Visser et al., 2010).

The most remarkable cortico-cortical connection in term of fiber density and anisotropy was constituted by the two longitudinal fasciculi: (1) the middle longitudinal fasciculus (mLF) that links the inferior parietal lobe including the angular gyrus (BA39) and posterior part of the superior temporal gyrus (BA22) to the superior (BA38) and middle (BA21) temporal gyri and (2) the inferior longitudinal fasciculus (iLF) that links the parahippocampus gyrus to the middle and superior temporal cortices (BA21 and BA38). Even though the WM fibers of these two longitudinal streams were intermingled, we could differentiate these 2 streams based on their different ROIs and their posterior trajectory in the temporal lobe. In the right hemisphere, we found similar tracts implicating the iLF that connects the inferior parietal cortex and the anterior part of the middle temporal gyrus BA21. Interestingly, these ventral pathways including the left mLF and the bilateral iLF were found with the highest factor of anisotropy revealing the WM integrity and efficiency.

Importantly, the imageability score provided when the subject was reading a sentence was significantly correlated with the factor of anisotropy of the left parieto-temporal connections of the mLF. The imageability score reflects the ability of the subject to form a mental image and the higher this imageability rating the more vivid are the simulated events evoked by the sentence. In a previous study, we have shown that this imageability rating is dependent on the context of the narrative and might reflect comprehension ability (Madden-Lombardi et al., 2015). Thus this relation between behaviour and connectivity rating is suggestive of the importance of the left ventral parieto-temporal pathways in semantic processing. While the factor of anisotropy of the mLF was significantly correlated with the imageability score, we did not observe a significant correlation with imageability and fiber density as previously observed (Jouen et al., 2015). This difference might result from the different tractography methods. Indeed, in our previous neuroimaging study, we use a deterministic tractography analysis of the ensemble of connections between the parietal and temporal cortex that could have included passing fibers. In the current approach, each WM bundle was determined by counting only the fibers terminating in the two selected ROIs. This restrictive analysis of the WM pathways is likely

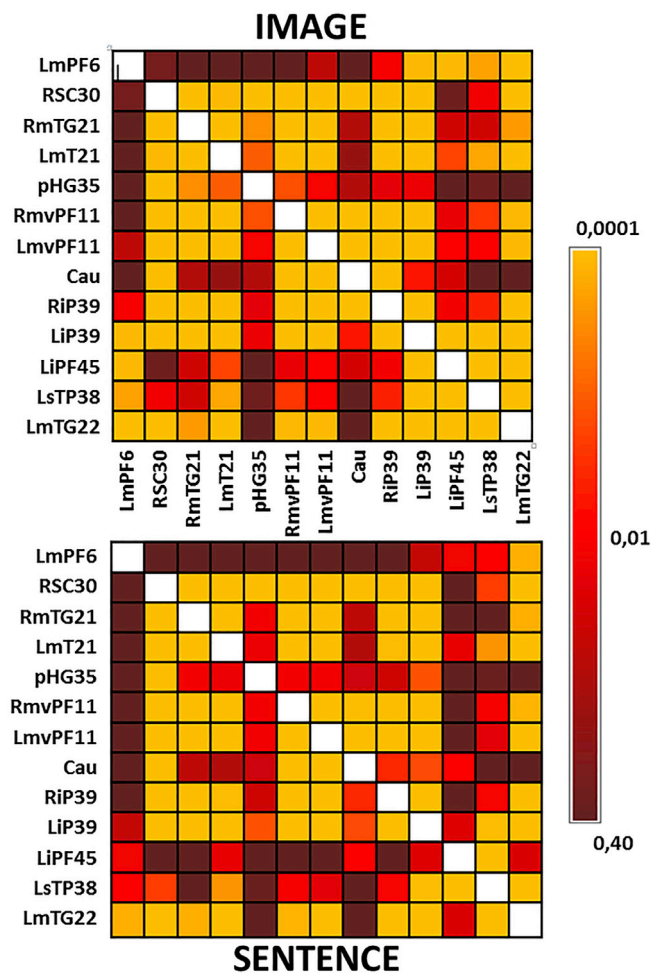


Fig. 6. p values matrices for the pairwise marginal correlations between the 13 ROIs of the semantic network activated during the image and sentence tasks. Note the similarity between the patterns of the marginal correlations in the two conditions. The anatomical sites are indicated with their corresponding Brodman's area. LiP and RiP: Left and right inferior parietal cortex - RSC: retrosplenial cortex - LmT and RmT: Left and right middle temporal cortex - LsTP: Left superior temporal pole - LpH: Left parahippocampus cortex - LiPF: Left inferior prefrontal cortex - LmPF: Left middle prefrontal cortex - LvmPF and RvmPF: Left and right ventro-medial prefrontal cortex - Caud: Caudate nucleus.

to provide more robust and selective information in terms of the structural correlates of our semantic network connectivity. With these new more precise measures, we identified a correlation between the factor of anisotropy of the mLF and the imageability score, thus confirming our previous finding of a link between imageability and parieto-temporal connectivity.

As part of the posterior cortico-cortical connectivity, we observed fibers located in the posterior WM cingulum pathway connecting the retrosplenial cortex (posterior grey matter cingulum) and the parahippocampal cortex. Even though the bundles were not as dense as the longitudinal fasciculi, they were found in the majority of subjects. As we know, the retrosplenial cortex is part of the medial structures that belong to the resting-state network involved in introspective processing and conceptual operations (Laird et al., 2009; Regen et al., 2016; Vann et al., 2009). The role of these temporo-cingular pathways will be developed further by considering the functional connectivity.

Another important bundle connecting the anterior temporal pole to the prefrontal cortex was the uncinate fasciculus (UF). From the anterior temporal pole the UF formed a loop of WM fibers reaching the prefrontal cortex into two branches: a lateral branch to the inferior prefrontal cortex and a medial branch to the ventro-medial prefrontal cortex. In our previous neuroimaging study (Jouen et al., 2015) we suggested that the

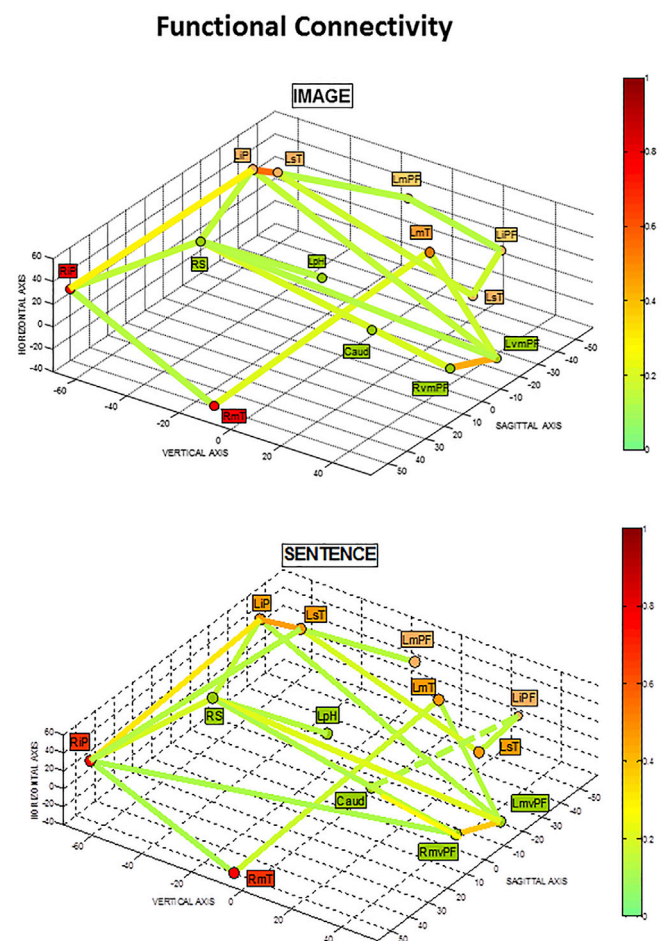


Fig. 7. Network graphs showing the degree of functional interactivities based on partial correlations coefficients for the 13 ROIs of the semantic network activated during image and sentence conditions. Only the significant links (p corrected < 0.05) are represented. Note the similarity between the functional interactions patterns obtained in the two conditions. LiP and RiP: Left and right inferior parietal cortex - RSC: retrosplenial cortex - LmT and RmT: Left and right middle temporal cortex - LsT: Left superior temporal cortex - LpH: Left parahippocampus cortex - LiPF: Left inferior prefrontal cortex - LmPF: Left middle prefrontal cortex - LvmPF and RvmPF: Left and right ventro-medial prefrontal cortex - Caud: Caudate nucleus.

inferior prefrontal cortex and the caudate nucleus might be responsible for controlling conceptual knowledge common to language and visual systems. In addition, the role of the inferior frontal cortex located rostrally in pars triangularis has been involved in semantic control including selection and working memory (Jefferies, 2013; Thompson-Schill, 2003; Zahr et al., 2009) independently of the stimulus modality. Likewise, the UF laterally interconnecting the anterior temporal cortex and the inferior frontal cortex has been involved in semantic cognition (Binney et al., 2012) and in semantic control during word comprehension (Harvey et al., 2013). By combining two DTI and resting-state fMRI neuroimaging techniques with neuropsychological investigations of aphasic patients, Harvey et al., (2013) found an association between the structural integrity of the UF and performance on behavioural measures of semantic control. Besides the inferior prefrontal cortex, the UF consistently linked the anterior temporal cortex to the ventro-medial prefrontal cortex. The orbito-frontal cortex has been implicated in behavioural- and social-related cognition (Feldmanhall et al., 2014; Lewis et al., 2005, 2011; Moll et al., 2011) as well as self-reference processing and self-knowledge involving the default-mode network (Molnar-Szakacs and Uddin, 2013). Furthermore, our results demonstrate that the ventro-medial orbito-frontal cortex also receives connections via the thalamic radiations from the striatum. Likewise, Han

et al., (2013) reported that the left anterior thalamic radiations constitute a necessary pathway for semantic processing. Complementary to these observations we found in some subjects WM fibers of the UF connecting the caudate nucleus and the anterior temporal cortex. These findings are consistent with the idea that the striatum including the caudate nucleus regulates semantically related operations (Crosson et al., 2007). Taken together these prefrontal tracts including uncinate fasciculus and thalamic radiations constitute a structural pattern of temporo-fronto-striatal connections carrying the lexical-semantic information necessary for executive control. In contrast to some authors (Almairac et al., 2015; Han et al., 2013; Moritz-Gasser et al., 2013; 2015), we did not isolate direct connections through the inferior fronto-occipital fasciculus (iFOF) that links the posterior temporal and occipital cortex and the prefrontal cortex. Duffau and colleagues (Almairac et al., 2015; Duffau, 2005; Duffau et al., 2013; Moritz-Gasser et al., 2013) proposed a dynamic dual-route model made of a direct crucial stream, the iFOF involved in the awareness of amodal semantic knowledge and an indirect compensatory stream centered on the temporal lobe including iLF/mLF and UF involved in semantic processing as previously described. These contrasting observations might arise from the location and size of our prefrontal cortical seeds (ROIs) based on previously defined small clusters in the inferior and ventro-medial prefrontal cortices which were activated during both sentence and picture presentation (Jouen et al., 2015).

Overall, this pattern of structural connections forming a large-scale ventral network provides compelling evidence for at least one major node in the anterior part of the superior temporal gyrus. Indeed, this anterior temporal region, despite its small size is the locus of convergence/divergence of several pathways coming from the inferior parietal and posterior temporal cortex, the retrosplenial cortex, the inferior and ventro-medial prefrontal cortex and the striatum. Consistent with the literature, our findings suggest the existence of a “semantic hub” localised in the anterior part of the superior temporal lobe.

Functional subsets inside the semantic network

When considering the functional relations between the nodes of our semantic network, evidence is provided of sub-systems differently implicated in semantic computation. In fact, such meaning processes requires the interplay of cognitive functions, i.e. bottom-up encoding operations linked to embodied sensory-motor simulation, heteromodal binding and integration, amodal representation, semantic memory and executive control as well as interoceptive activities, episodic memory and self-referenced operations. In this context, our functional analysis provides empirical evidence for specific patterns of co-activated neural structures that will trigger semantic related operations. Interestingly, apart from few modality specific interactions, these patterns of co-activated nodes were very similar for the two semantic networks extracted from the picture and sentence comprehension tasks. Based on the literature and our structural and functional data, we distinguish two sub-networks differently distributed: (1) one forming lateral interactions between inferior parietal, superior and middle temporal and inferior and middle prefrontal cortex and including the peri-sylvian region and (2) another one forming medial interactions between the retrosplenial, parahippocampus, ventro-medial prefrontal cortex and striatum.

A lateral parieto-temporal hub centered network:

When considering the parieto-temporo-prefrontal functional connectivity, the first striking observation is the lateral localisation of the cortical structures and their links at least partially with sensory-motor representation. As mentioned above, semantic processing is grounded in the brain's sensory and motor systems with information converging in heteromodal associations cortices (Barsalou, 2008; Binder et al., 2016; Damasio, 1989; Fernandino et al., 2016a, 2016c; Jouen et al., 2015; Mahon and Hickok, 2016; Man et al., 2013; Meyer and Damasio, 2009; Pulvermuller et al., 2005). This embodied theory of comprehension postulates that the meaning of action is grounded in the internal

simulation of one's own sensori-motor experience. Thereby the understanding of others' actions relies on the internal replay of one's own actions implicating the observation/action “mirror-neuron” system in humans (Gallese et al., 1996; Rizzolatti and Craighero, 2004; Rizzolatti et al., 1996, 2001). For example, seeing another's hand grasping an object will activate premotor and associative brain regions, including the inferior parietal cortex in conjunction with the premotor cortex. Such an embodied representation of meaning should serve for multiple modalities including other perceptual states, emotion, and language. In our study, we recall that each event described an action executed by at least one person (e.g., running, eating, climbing). According to embodied theories, the subject understands the picture or sentence at least in part by simulating the event evoked by the stimuli. Accordingly, the significant coactivation found in our study between the left parieto-temporal cluster and the middle prefrontal cortex (BA6) implicated in premotor computations, might correspond to the neural underpinning of the semantic analysis through sensory-motor grounded representations of seen or read events. In addition to these observations, the inferior parietal cortex including the angular gyrus has been considered as a candidate region that might support the convergence of multiple modality-specific semantic operations (Bonner et al., 2013; Fernandino et al., 2016a, 2016c; Molinaro et al., 2015; Price et al., 2015). In our network spanning the two hemispheres, the inferior parietal nodes were tightly interconnected, and were connected with the posterior part of the superior temporal gyrus (BA22) at the highest correlation rate. Partially overlapping the semantic Wernicke's area on the left side, these parieto-temporal regions have a key location as they are at the crossroads of auditory and visual inputs. Interestingly the lateral peri-sylvian functional subcomponent of our semantic network associates the inferior parietal cortex and the rostral temporal site linked to the inferior prefrontal cortex via the uncinate fasciculus as described above. While the temporal lobe brings together modality specific representations of verbal and non-verbal features along a caudo-rostral gradient, the anterior pole of the superior temporal gyrus might serve to compile and store the concept representation in an amodal format (Binder et al., 2009; Binney et al., 2012; Hoffman et al., 2015; Lambon Ralph et al., 2017; Patterson et al., 2007; Rice et al., 2015; Visser et al., 2010). Accordingly, Molinaro et al., (2015) emphasize the dynamics of these left perisylvian regions during semantic combinatorial operations. These authors suggest that the strong positive coupling between anterior temporal cortex and angular gyrus is necessary to access the rich amodal representations stored in semantic memory.

In accordance with this literature, our findings bring further insights on the neural semantic framework as we demonstrate an effective functional connectivity forming several interactive sub-systems including (a) a premotor, inferior parietal and posterior temporal loop likely involved in modality-specific encoding and binding, (b) an inferior parietal and superior temporal coactivation underlying the access to transmodal representation and storing and finally (c) a superior temporal and inferior prefrontal interaction involved in semantic control. As a whole the laterally distributed connectivity will be responsible for a conceptual representation of the external world involving both parietal and temporal centers under the executive control of the prefrontal cortico-striatal system and the uncinate connections. Moreover, while the temporo-parietal cortex is part of the lateral neural network, it might also constitute a key interface with the medial sub-component of our semantic network.

A medial retrosplenial hub centered network:

In contrast to the lateral network, the medial semantic functional connectivity largely overlapped the default-mode network (DMN) that has been described in several previous fMRI resting state studies (Fransson and Marrelec, 2008; Gusnard et al., 2001; Molnar-Szakacs and Uddin, 2013; Raichle et al., 2001). The DMN is involved in introspection and internal world operations including episodic memory, memory consolidation, representation of self and others, and socio-emotional cognition (Buckner et al., 2008; Gusnard et al., 2001; Laird et al.,

2011; Northoff et al., 2006; Raichle et al., 2001). In the proposed intrinsic sub-network, it is noteworthy that the majority of the functional interactions converges onto the associative visual region of the retrosplenial cortex (RSC) located in the posterior cingulate cortex. Bilaterally linked to the inferior parietal cortex, this RSC might constitute a functional node for a set of medial neural structures including the ventro-medial prefrontal cortex bilaterally and the left parahippocampus. By using a similar IC analysis, Fransson and Marrelec (Fransson and Marrelec, 2008) characterised an effective connectivity based on partial correlations inside the DMN, that is comparable to our semantic network. Pertinent with our findings, these authors describe the posterior cingulate cortex as a pivotal role in how the intrinsic activity is mediated throughout the DMN. Furthermore, there is compelling evidence from neuroimaging and clinical studies that the RSC might have a key role in scene construction underpinning autobiographical memory, as well as navigation and thinking of future scenarios [for review see (Vann et al., 2009)]. Accordingly, we found a substantial link through both structural and functional connections between the RSC and parahippocampal cortex involved in episodic memory. Based on its consistent anatomical relation with the hippocampal region, the RSC has been associated with a “translational function” by transforming spatial frames of reference during mental imagery. Thus, the hippocampal cortex might encode imagined or memorized spatial information and the RSC will transform this information into an egocentric representation so that the autobiographical memory, scene or imagined event can be viewed from a different perspective. In this context, we observe synchronised activity patterns bilaterally between the parahippocampus gyrus, RSC, ventro-medial prefrontal and inferior parietal nodes thereby realising a complete recurrent circuit. Another important site in the default-mode network is the ventro-medial prefrontal cortex which is associated with emotional engagement, social interactions and morality (Li et al., 2014). As discussed above, the ventro-medial prefrontal cortex was part of the medial functional network including the RSC and linked to the inferior parietal cortex bilaterally. If such a fronto-cingulate-temporo-parietal circuit is significantly implicated in our study, we can ask “which are the cognitive processes triggered by our experimental tasks that might explain the coactivation of these medial structures?” During the semantic analysis of the event evoked by our pictures or sentences (persons engaged in everyday actions), the participant will recognize and interpret the situation through several cognitive operations: self-projection in the scene, recall from episodic memory and Theory of Mind (ToM). ToM has been described as the ability to attribute affective and cognitive mental states to others in order to comprehend their intention or behaviour (Carrington and Bailey, 2009). These cognitive functions underlying the understanding of others' actions, intentions, or feelings will at least partially trigger the default-mode network i.e. the hippocampus and parahippocampal cortex, the RSC and the ventro-medial prefrontal cortex.

Our findings describing functional connectivity in our semantic network support the idea of two complementary and interacting sub-systems forming distributed networks: one involving lateral brain structures interacting with external information and the other involving medial brain structures associated with self-relevant processes which will serve for understanding the environmental state, including others. The parieto-temporal cortex including the angular gyri in the two hemispheres might constitute a hub region of interactions between the two medial and lateral networks ensuring heteromodal and combinatorial semantic processes.

Considerations on a unified view of the semantic neural system

The anatomical and functional network that we describe in the context of understanding sentences and images provides insight into current opinions on the nature of the distributed semantic system. Our analysis revealed highly coactivated nodes, both in the anterior temporal lobe (BA38) and in the region of the temporo-parietal cortex (BA39)

suggesting dual and cooperating roles for these areas within the semantic system. In this integrated framework the anterior temporal lobe serves as a cross-modal hub that encodes semantic similarity (Chen et al., 2017), and is abstracted away from grounded sensory-motor embodied representations. These more embodied sensorimotor simulations are implemented in parietal areas including the angular gyrus (Binder and Desai, 2011; Binder et al., 2009) and temporo-parietal cortex as part of a general semantic network that encodes multimodal information derived from basic sensory-motor processes (Fernandino et al., 2016b). Interestingly, this more embodied dimension of the semantic system is partially captured in the notion of praxis and function features that are associated with parietal regions including pMTG (Chen et al., 2017). The anatomical and functional characterization of a semantic network that serves in the comprehension of sentences and visual scenes thus provides a framework that encompasses these complementary roles for the anterior temporal lobe and the parietal cortex.

Conclusions

By providing complementary results on the activated sites and their connections during semantic analysis, this research yields a general framework of the functional processes and structural organisation underpinning semantic analysis. The major connections of white matter fibers link ventral neural structures including the parietal and temporal cortices through inferior and middle longitudinal fasciculi, the temporal and parahippocampal gyrus through the cingulate bundle, and the temporal and prefrontal structures through the uncinate fasciculus. Part of this structural connectivity corresponds to functional interactions between principal nodes including the anterior temporal pole, the parietal (angular gyrus) and frontal cortices. Based on the functional correlations, we distinguish two semantical related sub-systems (1) one lateral involving laterally localized connectivity that will be responsible for a conceptual representation of the external world and (2) another one medial involving medially localized connectivity that will be responsible for introspection process and conceptual representation of self interacting with the external world through the lateral network, including the parieto-temporal cortex.

Funding

This work was supported by the French National Research Agency (ANR Project “Comprendre” and “Spaquence”) and by the European Community (EU FP7 Project “Wysiywd”).

Acknowledgements

The authors are grateful to Vincent Perlberg for his helpful comments during data analysis with the Netbrainwork toolbox.

Appendix A. Supplementary data

Supplementary data related to this article can be found at <https://doi.org/10.1016/j.neuroimage.2017.10.039>.

References

- Almairac, F., Herbet, G., Moritz-Gasser, S., de Champfleury, N.M., Duffau, H., 2015. The left inferior fronto-occipital fasciculus subserves language semantics: a multilevel lesion study. *Brain Struct. Funct.* 220, 1983–1995.
- Barsalou, L.W., 2008. Grounded cognition. *Annu. Rev. Psychol.* 59, 617–645.
- Basser, P.J., Pajevic, S., Pierpaoli, C., Duda, J., Aldroubi, A., 2000. In vivo fiber tractography using DT-MRI data. *Magnetic Reson. Med. Official J. Soc. Magnetic Reson. Med./Soc. Magnetic Reson. Med.* 44, 625–632.
- Binder, J.R., Conant, L.L., Humphries, C.J., Fernandino, L., Simons, S.B., et al., 2016. Toward a brain-based componential semantic representation. *Cogn. Neuropsychol.* 33, 130–174.
- Binder, J.R., Desai, R.H., 2011. The neurobiology of semantic memory. *Trends Cogn. Sci.* 15, 527–536.

- Binder, J.R., Desai, R.H., Graves, W.W., Conant, L.L., 2009. Where is the semantic system? A critical review and meta-analysis of 120 functional neuroimaging studies. *Cereb. Cortex* 19, 2767–2796.
- Binney, R.J., Parker, G.J., Lambon Ralph, M.A., 2012. Convergent connectivity and graded specialization in the rostral human temporal lobe as revealed by diffusion-weighted imaging probabilistic tractography. *J. Cognitive Neurosci.* 24, 1998–2014.
- Bonner, M.F., Peelle, J.E., Cook, P.A., Grossman, M., 2013. Heteromodal conceptual processing in the angular gyrus. *NeuroImage* 71, 175–186.
- Bozeat, S., Lambon Ralph, M.A., Patterson, K., Garrard, P., Hodges, J.R., 2000. Non-verbal semantic impairment in semantic dementia. *Neuropsychologia* 38, 1207–1215.
- Buckner, R.L., Andrews-Hanna, J.R., Schacter, D.L., 2008. The brain's default network: anatomy, function, and relevance to disease. *Ann. N. Y. Acad. Sci.* 1124, 1–38.
- Carrington, S.J., Bailey, A.J., 2009. Are there theory of mind regions in the brain? A review of the neuroimaging literature. *Hum. Brain Mapp.* 30, 2313–2335.
- Catani, M., Jones, D.K., ffytche, D.H., 2005. Perisylvian language networks of the human brain. *Ann. Neurol.* 57, 8–16.
- Catani, M., Thiebaut de Schotten, M., 2008. A diffusion tensor imaging tractography atlas for virtual in vivo dissections. *Cortex; a J. Devoted study Nerv. Syst. Behav.* 44, 1105–1132.
- Chen, L., Ralph, M.A.L., Rogers, T.T., 2017. A unified model of human semantic knowledge and its disorders. *Nat. Hum. Behav.* 1.
- Cox, R.W., 1996. AFNI: software for analysis and visualization of functional magnetic resonance neuroimages. *Comput. Biomed. Res. Int. J.* 29, 162–173.
- Coyne, D., Marrelec, G., Perlberg, V., Pelegrini-Issac, M., Van de Moortele, P.F., et al., 2010. Dynamics of motor-related functional integration during motor sequence learning. *NeuroImage* 49, 759–766.
- Crosson, B., Benjamin, M., Levy, I., 2007. Role of the basal ganglia in language and semantics: supporting cast. *Neural Basis Semantic Mem.* 219–245.
- Damasio, A.R., 1989. Time-locked multiple regional retroactivation: a systems-level proposal for the neural substrates of recall and recognition. *Cognition* 33, 25–62.
- De Witt Hamer, P.C., Moritz-Gasser, S., Gatignol, P., Duffau, H., 2011. Is the human left middle longitudinal fascicle essential for language? A brain electrostimulation study. *Hum. Brain Mapp.* 32, 962–973.
- Duffau, H., 2005. Intraoperative cortico-subcortical stimulations in surgery of low-grade gliomas. *Expert Rev. Neurother.* 5, 473–485.
- Duffau, H., Herbet, G., Moritz-Gasser, S., 2013. Toward a pluri-component, multimodal, and dynamic organization of the ventral semantic stream in humans: lessons from stimulation mapping in awake patients. *Front. Syst. Neurosci.* 7, 44.
- Ellmore, T.M., Beauchamp, M.S., Breier, J.I., Slater, J.D., Kalamangalam, G.P., et al., 2010. Temporal lobe white matter asymmetry and language laterality in epilepsy patients. *NeuroImage* 49, 2033–2044.
- Fang, Y., Han, Z., Zhong, S., Gong, G., Song, L., et al., 2015. The semantic anatomical network: evidence from healthy and brain-damaged patient populations. *Hum. Brain Mapp.* 36, 3499–3515.
- Feldmanhall, O., Mobbs, D., Dalgleish, T., 2014. Deconstructing the brain's moral network: dissociable functionality between the temporoparietal junction and ventromedial prefrontal cortex. *Soc. Cognitive Affect. Neurosci.* 9, 297–306.
- Fernandino, L., Binder, J.R., Desai, R.H., Pendl, S.L., Humphries, C.J., et al., 2016a. Concept representation reflects multimodal abstraction: a framework for embodied semantics. *Cereb. Cortex* 26, 2018–2034.
- Fernandino, L., Humphries, C.J., Conant, L.L., Seidenberg, M.S., Binder, J.R., 2016b. Heteromodal cortical areas encode sensory-motor features of word meaning. *J. Neurosci.* 36, 9763–9769.
- Fernandino, L., Humphries, C.J., Conant, L.L., Seidenberg, M.S., Binder, J.R., 2016c. Heteromodal cortical areas encode sensory-motor features of word meaning. *J. Neurosci. Official J. Soc. Neurosci.* 36, 9763–9769.
- Floel, A., de Vries, M.H., Scholz, J., Breitenstein, C., Johansen-Berg, H., 2009. White matter integrity in the vicinity of Broca's area predicts grammar learning success. *NeuroImage* 47, 1974–1981.
- Fransson, P., Marrelec, G., 2008. The precuneus/posterior cingulate cortex plays a pivotal role in the default mode network: evidence from a partial correlation network analysis. *NeuroImage* 42, 1178–1184.
- Gallese, V., Fadiga, L., Fogassi, L., Rizzolatti, G., 1996. Action recognition in the premotor cortex. *Brain a J. Neurol.* 119 (Pt 2), 593–609.
- Geranmayeh, F., Leech, R., Wise, R.J., 2015. Semantic retrieval during overt picture description: left anterior temporal or the parietal lobe? *Neuropsychologia* 76, 125–135.
- Glasser, M.F., Rilling, J.K., 2008. DTI tractography of the human brain's language pathways. *Cereb. Cortex* 18, 2471–2482.
- Guo, C.C., Gorno-Tempini, M.L., Gesierich, B., Henry, M., Trujillo, A., et al., 2013. Anterior temporal lobe degeneration produces widespread network-driven dysfunction. *Brain a J. Neurol.* 136, 2979–2991.
- Gusnard, D.A., Akbudak, E., Shulman, G.L., Raichle, M.E., 2001. Medial prefrontal cortex and self-referential mental activity: relation to a default mode of brain function. *Proc. Natl. Acad. Sci. U. S. A.* 98, 4259–4264.
- Hagmann, P., Cammoun, L., Martuzzi, R., Maeder, P., Clarke, S., et al., 2006. Hand preference and sex shape the architecture of language networks. *Hum. Brain Mapp.* 27, 828–835.
- Han, Z., Ma, Y., Gong, G., He, Y., Caramazza, A., Bi, Y., 2013. White matter structural connectivity underlying semantic processing: evidence from brain damaged patients. *Brain a J. Neurol.* 136, 2952–2965.
- Harvey, D.Y., Wei, T., Ellmore, T.M., Hamilton, A.C., Schnur, T.T., 2013. Neuropsychological evidence for the functional role of the uncinate fasciculus in semantic control. *Neuropsychologia* 51, 789–801.
- Hickok, G., Poeppel, D., 2004. Dorsal and ventral streams: a framework for understanding aspects of the functional anatomy of language. *Cognition* 92, 67–99.
- Hoffman, P., Binney, R.J., Lambon Ralph, M.A., 2015. Differing contributions of inferior prefrontal and anterior temporal cortex to concrete and abstract conceptual knowledge. *Cortex; a J. Devoted study Nerv. Syst. Behav.* 63, 250–266.
- Jackson, R.L., Hoffman, P., Pobric, G., Lambon Ralph, M.A., 2016. The semantic network at work and rest: Differential connectivity of anterior temporal lobe subregions. *J. Neurosci. Official J. Soc. Neurosci.* 36, 1490–1501.
- Jefferies, E., 2013. The neural basis of semantic cognition: converging evidence from neuropsychology, neuroimaging and TMS. *Cortex; a J. Devoted Study Nerv. Syst. Behav.* 49, 611–625.
- Jefferies, E., Lambon Ralph, M.A., 2006. Semantic impairment in stroke aphasia versus semantic dementia: a case-series comparison. *Brain a J. Neurol.* 129, 2132–2147.
- Jouen, A.L., Ellmore, T.M., Madden, C.J., Pallier, C., Dominey, P.F., Ventre-Dominey, J., 2015. Beyond the word and image: characteristics of a common meaning system for language and vision revealed by functional and structural imaging. *NeuroImage* 106, 72–85.
- Jung, J., Cloutman, L.L., Binney, R.J., Lambon Ralph, M.A., 2016. The structural connectivity of higher order association cortices reflects human functional brain networks. *Cortex. in press (online, https://doi.org/10.1016/j.cortex.2016.08.011).*
- Laird, A.R., Eickhoff, S.B., Li, K., Robin, D.A., Glahn, D.C., Fox, P.T., 2009. Investigating the functional heterogeneity of the default mode network using coordinate-based meta-analytic modeling. *J. Neurosci. Official J. Soc. Neurosci.* 29, 14496–14505.
- Laird, A.R., Fox, P.M., Eickhoff, S.B., Turner, J.A., Ray, K.L., et al., 2011. Behavioral interpretations of intrinsic connectivity networks. *J. Cognitive Neurosci.* 23, 4022–4037.
- Lambon Ralph, M.A., 2014. Neurocognitive insights on conceptual knowledge and its breakdown. *Philosophical Trans. R. Soc. Lond. Ser. B, Biol. Sci.* 369, 20120392.
- Lambon Ralph, M.A., Jefferies, E., Patterson, K., Rogers, T.T., 2017. The neural and computational bases of semantic cognition. In: *Nature Reviews Neuroscience*, pp. 42–54.
- Le Bihan, D., Breton, E., Lallemand, D., Grenier, P., Cabanis, E., Laval-Jeantet, M., 1986. MR imaging of intravoxel incoherent motions: application to diffusion and perfusion in neurologic disorders. *Radiology* 161, 401–407.
- Leemans, A., Jones, D.K., 2009. The B-matrix must be rotated when correcting for subject motion in DTI data. *Magnetic Reson. Med. Official J. Soc. Magnetic Reson. Med./Soc. Magnetic Reson. Med.* 61, 1336–1349.
- Lewis, P.A., Critchley, H.D., Smith, A.P., Dolan, R.J., 2005. Brain mechanisms for mood congruent memory facilitation. *NeuroImage* 25, 1214–1223.
- Lewis, P.A., Rezaie, R., Brown, R., Roberts, N., Dunbar, R.I., 2011. Ventromedial prefrontal volume predicts understanding of others and social network size. *NeuroImage* 57, 1624–1629.
- Li, W., Mai, X., Liu, C., 2014. The default mode network and social understanding of others: what do brain connectivity studies tell us. *Front. Hum. Neurosci.* 8, 74.
- Madden-Lombardi, C., Jouen, A.L., Dominey, P.F., Ventre-Dominey, J., 2015. Sequential Coherence in Sentence Pairs Enhances Imagery during Comprehension: an individual differences study. *PLoS one* 10, e0138269.
- Mahon, B.Z., Hickok, G., 2016. Arguments about the nature of concepts: symbols, embodiment, and beyond. *Psychonomic Bull. Rev.* 23, 941–958.
- Makris, N., Pandya, D.N., 2009. The extreme capsule in humans and rethinking of the language circuitry. *Brain Struct. Funct.* 213, 343–358.
- Makris, N., Papadimitriou, G.M., Kaiser, J.R., Sorg, S., Kennedy, D.N., Pandya, D.N., 2009. Delineation of the middle longitudinal fascicle in humans: a quantitative, in vivo, DT-MRI study. *Cereb. Cortex* 19, 777–785.
- Makris, N., Zhu, A., Papadimitriou, G.M., Mouradian, P., Ng, I., et al., 2017. Mapping temporo-parietal and temporo-occipital cortico-cortical connections of the human middle longitudinal fascicle in subject-specific, probabilistic, and stereotaxic Talairach spaces. *Brain imaging Behav.* 11, 1258–1277.
- Man, K., Kaplan, J., Damasio, H., Damasio, A., 2013. Neural convergence and divergence in the mammalian cerebral cortex: from experimental neuroanatomy to functional neuroimaging. *J. Comp. Neurol.* 521, 4097–4111.
- Marrelec, G., Bellec, P., Krainik, A., Duffau, H., Pelegrini-Issac, M., et al., 2008. Regions, systems, and the brain: hierarchical measures of functional integration in fMRI. *Med. Image Anal.* 12, 484–496.
- Martino, J., Brogna, C., Robles, S.G., Vergani, F., Duffau, H., 2010. Anatomic dissection of the inferior fronto-occipital fasciculus revisited in the lights of brain stimulation data. *Cortex; a J. Devoted study Nerv. Syst. Behav.* 46, 691–699.
- Meyer, K., Damasio, A., 2009. Convergence and divergence in a neural architecture for recognition and memory. *Trends Neurosci.* 32, 376–382.
- Molinero, N., Paz-Alonso, P.M., Dunabeitia, J.A., Carreiras, M., 2015. Combinatorial semantics strengthens angular-anterior temporal coupling. *Cortex; a J. Devoted study Nerv. Syst. Behav.* 65, 113–127.
- Moll, J., Zahn, R., de Oliveira-Souza, R., Bramati, I.E., Krueger, F., et al., 2011. Impairment of prosocial sentiments is associated with frontopolar and septal damage in frontotemporal dementia. *NeuroImage* 54, 1735–1742.
- Molnar-Szakacs, I., Uddin, L.Q., 2013. Self-processing and the default mode network: interactions with the mirror neuron system. *Front. Hum. Neurosci.* 7, 571.
- Moritz-Gasser, S., Herbet, G., Duffau, H., 2013. Mapping the connectivity underlying multimodal (verbal and non-verbal) semantic processing: a brain electrostimulation study. *Neuropsychologia* 51, 1814–1822.
- Moritz-Gasser, S., Herbet, G., Duffau, H., 2015. Integrating emotional valence and semantics in the human ventral stream: a hodological account. *Front. Psychol.* 6, 32.
- Nichols, T., Brett, M., Andersson, J., Wager, T., Poline, J.B., 2005. Valid conjunction inference with the minimum statistic. *NeuroImage* 25, 653–660.
- Noonan, K.A., Jefferies, E., Corbett, F., Lambon Ralph, M.A., 2010. Elucidating the nature of deregulated semantic cognition in semantic aphasia: evidence for the roles of prefrontal and temporo-parietal cortices. *J. Cognitive Neurosci.* 22, 1597–1613.

- Northoff, G., Heinzel, A., de Greck, M., Bempohl, F., Dobrowolny, H., Panksepp, J., 2006. Self-referential processing in our brain—a meta-analysis of imaging studies on the self. *NeuroImage* 31, 440–457.
- Parker, G.J., Luzzi, S., Alexander, D.C., Wheeler-Kingshott, C.A., Ciccarelli, O., Lambon Ralph, M.A., 2005. Lateralization of ventral and dorsal auditory-language pathways in the human brain. *NeuroImage* 24, 656–666.
- Patterson, K., Nestor, P.J., Rogers, T.T., 2007. Where do you know what you know? The representation of semantic knowledge in the human brain. *Nat. Rev. Neurosci.* 8, 976–987.
- Perlberg, V., Marrelec, G., 2008. Contribution of exploratory methods to the investigation of extended large-scale brain networks in functional MRI: methodologies, results, and challenges. *Int. J. Biomed. Imaging* 2008, 218519.
- Perlberg, V., Marrelec, G., Bellec, P., Coynel, D., Pélégrini-Issac, M., Benali, H., 2009. NetBrainWork: a toolbox for studying functional interactions in large-scale brain networks in fMRI. *NeuroImage* 47.
- Perlberg, V., Marrelec, G., Doyon, J., Pélégrini-Issac, M., Lehericy, S., Benali, H., 2008. NEDICA: Detection of group functional networks in fMRI using spatial independent component analysis. In: *Biomedical Imaging From Nano to Macro*, 2008. ISBI 2008. 5th IEEE International Symposium, pp. 1247–1250.
- Pobric, G., Jefferies, E., Ralph, M.A., 2010. Amodal semantic representations depend on both anterior temporal lobes: evidence from repetitive transcranial magnetic stimulation. *Neuropsychologia* 48, 1336–1342.
- Powell, H.W., Parker, G.J., Alexander, D.C., Symms, M.R., Boulby, P.A., et al., 2006. Hemispheric asymmetries in language-related pathways: a combined functional MRI and tractography study. *NeuroImage* 32, 388–399.
- Price, A.R., Bonner, M.F., Peelle, J.E., Grossman, M., 2015. Converging evidence for the neuroanatomic basis of combinatorial semantics in the angular gyrus. *J. Neurosci. Official J. Soc. Neurosci.* 35, 3276–3284.
- Pulvermuller, F., Hauk, O., Nikulin, V.V., Ilmoniemi, R.J., 2005. Functional links between motor and language systems. *Eur. J. Neurosci.* 21, 793–797.
- Raichle, M.E., MacLeod, A.M., Snyder, A.Z., Powers, W.J., Gusnard, D.A., Shulman, G.L., 2001. A default mode of brain function. *Proc. Natl. Acad. Sci. U. S. A.* 98, 676–682.
- Regen, W., Kyle, S.D., Nissen, C., Feige, B., Baglioni, C., et al., 2016. Objective sleep disturbances are associated with greater waking resting-state connectivity between the retrosplenial cortex/hippocampus and various nodes of the default mode network. *J. Psychiatr. Neurosci. JPN* 41, 295–303.
- Rice, G.E., Lambon Ralph, M.A., Hoffman, P., 2015. The roles of left versus right anterior temporal lobes in conceptual knowledge: an ALE meta-analysis of 97 functional neuroimaging studies. *Cereb. Cortex* 25, 4374–4391.
- Rizzolatti, G., Craighero, L., 2004. The mirror-neuron system. *Annu. Rev. Neurosci.* 27, 169–192.
- Rizzolatti, G., Fadiga, L., Gallese, V., Fogassi, L., 1996. Premotor cortex and the recognition of motor actions. *Brain Res. Cognitive Brain Res.* 3, 131–141.
- Rizzolatti, G., Fogassi, L., Gallese, V., 2001. Neurophysiological mechanisms underlying the understanding and imitation of action. *Nat. Rev. Neurosci.* 2, 661–670.
- Saur, D., Kreher, B.W., Schnell, S., Kummerer, D., Kellmeyer, P., et al., 2008. Ventral and dorsal pathways for language. *Proc. Natl. Acad. Sci. U. S. A.* 105, 18035–18040.
- Saur, D., Schelter, B., Schnell, S., Kratochvil, D., Kupper, H., et al., 2010. Combining functional and anatomical connectivity reveals brain networks for auditory language comprehension. *NeuroImage* 49, 3187–3197.
- Sherbondy, A., Akers, D., Mackenzie, R., Dougherty, R., Wandell, B., 2005. Exploring connectivity of the brain's white matter with dynamic queries. *IEEE Trans. Vis. Comput. Graph.* 11, 419–430.
- Talairach, J., Tournoux, P., 1988. *Co-planar Stereotaxic Atlas of the Human Brain : 3-dimensional Proportional System : an Approach to Cerebral Imaging*. Georg Thieme, Stuttgart; New York, 122 pp.
- Thompson-Schill, S.L., 2003. Neuroimaging studies of semantic memory: inferring “how” from “where”. *Neuropsychologia* 41, 280–292.
- Ueno, T., Saito, S., Rogers, T.T., Lambon Ralph, M.A., 2011. Lichtheim 2: synthesizing aphasia and the neural basis of language in a neurocomputational model of the dual dorsal-ventral language pathways. *Neuron* 72, 385–396.
- Vandenberghe, R., Price, C., Wise, R., Josephs, O., Frackowiak, R.S., 1996. Functional anatomy of a common semantic system for words and pictures. *Nature* 383, 254–256.
- Vann, S.D., Aggleton, J.P., Maguire, E.A., 2009. What does the retrosplenial cortex do? *Nat. Rev. Neurosci.* 10, 792–802.
- Visser, M., Jefferies, E., Ralph, M.L., 2010. Semantic processing in the anterior temporal lobes: a meta-analysis of the functional neuroimaging literature. *J. Cognitive Neurosci.* 22, 1083–1094.
- Visser, M., Lambon Ralph, M.A., 2011. Differential contributions of bilateral ventral anterior temporal lobe and left anterior superior temporal gyrus to semantic processes. *J. Cognitive Neurosci.* 23, 3121–3131.
- Wei, T., Liang, X., He, Y., Zang, Y., Han, Z., et al., 2012. Predicting conceptual processing capacity from spontaneous neuronal activity of the left middle temporal gyrus. *J. Neurosci. Official J. Soc. Neurosci.* 32, 481–489.
- Zahr, N.M., Rohlfing, T., Pfefferbaum, A., Sullivan, E.V., 2009. Problem solving, working memory, and motor correlates of association and commissural fiber bundles in normal aging: a quantitative fiber tracking study. *NeuroImage* 44, 1050–1062.